Contents

1

DRMG applied to two-dimensional classical lattice models

This chapter explains how to apply the ideas of the density matrix renormalization group to two-dimensional classical lattices.

First, we explain the transfer-matrix formulation for classical partition functions. Then, we show how to renormalize the transfer matrix using DMRG. This was first done by Nishino [1]. To make notation easier and up-to-date with current approaches, we redefine the transfer matrix in terms of a tensor network. Then, we explain the corner transfer matrix renormalization group (CTMRG) method. This method, first introduced by Nishino and Okunishi [2], unifies ideas from Baxter [3–5] and White [6] to significantly speed up the renormalization of the transfer matrix.

1.1 Statistical mechanics on classical lattices

For a general introduction to statistical mechanics, we refer to [7].

The central quantity in equilibrium statistical mechanics is the partition function Z, which, for a discrete system such as a lattice, is defined as

$$Z = \sum_s \exp\left(-\beta H(s)\right), \tag{1.1}$$

where the sum is over all microstates s, H is the energy function, and $\beta = T^{-1}$ the inverse temperature.

The probability that the system is in a particular microstate

$$p(s) = \frac{\exp(-\beta H(s))}{Z} \tag{1.2}$$

is also called the *Boltzmann weight*.

At first glance, the partition function is a simple normalization factor. But its importance stems from the fact that since it contains all statistical information about the system, all thermodynamic quantities can be expressed as a function of Z.

The energy of the system is expressed as

$$\langle E \rangle = \frac{\sum_s H(s) \exp(-\beta H(s))}{Z} = -\frac{\partial}{\partial \beta} \log Z, \tag{1.3}$$

the entropy as

$$S = -\sum_s p(s) \log p(s) = \frac{\partial}{\partial T}(T \log Z), \tag{1.4}$$

and the free energy as

$$F = \langle E \rangle - TS = T^2 \frac{\partial}{\partial T} \log Z - T \frac{\partial}{\partial T}(T \log Z) = -T \log Z. \tag{1.5}$$

1.2 Transfer matrices of lattice models

Transfer matrices are used to re-express the partition function of classical lattice systems, allowing them to be solved exactly or approximated.

We will introduce the transfer matrix in the context of the 1D classical Ising model, first introduced and solved using the transfer matrix method by Ising [8] in his PhD thesis.

1.2.1 1D Ising model

Consider the 1D ferromagnetic Ising model [8], defined by the energy function

$$H(\sigma) = -J \sum_{\langle ij \rangle} \sigma_i \sigma_j - h \sum_i \sigma_i. \tag{1.6}$$

Here, we sum over nearest neighbors $\langle ij \rangle$ and the spins σ_i take the values ± 1. $J > 0$ is the spin coupling and $h > 0$ an external magnetic field.

Assume, for the moment, that the chain consists of N spins, and apply periodic boundary conditions. The partition function of this system is given by

$$Z_N = \sum_{\sigma_1, \ldots, \sigma_N \in \{-1, 1\}} \exp(-\beta H(\sigma)) \tag{1.7}$$

Exploiting the local nature of the interaction between spins, we can write

$$Z_N = \sum_{\sigma_1,\cdots,\sigma_N \in \{-1,1\}} \prod_{\langle i,j \rangle} e^{K\sigma_i\sigma_j + \frac{H}{2}(\sigma_i+\sigma_j)} \tag{1.8}$$

where we defined $K \equiv \beta J$ and $H \equiv \beta h$.

Now, we define the 2×2 matrix

$$T_{\sigma\sigma'} = \exp(K\sigma\sigma' + \frac{H}{2}(\sigma + \sigma')). \tag{1.9}$$

for which a possible choice of basis is

$$(|\uparrow\rangle = 1, |\downarrow\rangle = -1) = (\begin{bmatrix}1\\0\end{bmatrix}, \begin{bmatrix}0\\1\end{bmatrix}). \tag{1.10}$$

In terms of this matrix, Z_N is written as

$$Z_N = \sum_{\sigma_1,\cdots,\sigma_N} T_{\sigma_1\sigma_2}\cdots T_{\sigma_N\sigma_1} = \mathrm{Tr}\, T^N. \tag{1.11}$$

T is called the transfer matrix. In the basis of Eq. 1.10, it is written as

$$T = \begin{bmatrix} e^{K+H} & e^{-K} \\ e^{-K} & e^{K-H} \end{bmatrix}. \tag{1.12}$$

T is, in fact, diagonalizable. So, we can write $T^N = PD^NP^{-1}$, where P consists of the eigenvectors of T, and D has the corresponding eigenvalues on the diagonal. By the cyclic property of the trace, we have

$$Z_N = \lambda_+^N + \lambda_-^N, \tag{1.13}$$

where

$$\lambda_\pm = e^K \left[\cosh(H) \pm \sqrt{\sinh^2(H) + e^{-4K}}\right] \tag{1.14}$$

Thus, we have reduced the problem of finding the partition function to an eigenvalue problem.

In the thermodynamic limit $N \to \infty$

$$Z = \lim_{N\to\infty} \lambda_+^N \tag{1.15}$$

where λ_+ is the non-degenerate largest eigenvalue (in absolute value) of T. Thermodynamic quantities like the free energy per site

$$\frac{F}{N} = -T \log \lambda_+ \tag{1.16}$$

and the magnetization per site

$$M = \frac{\sum_i^N \langle \sigma_i \rangle}{N} = -\frac{1}{N}\frac{\partial F}{\partial h} \tag{1.17}$$

can now readily be calculated.

1.2.1.1 Fixed boundary conditions

We may also apply fixed boundary conditions. The partition function is then written as

$$Z_N = \langle \sigma' | \, T^N \, | \sigma \rangle \,, \tag{1.18}$$

where $|\sigma\rangle$ and $|\sigma'\rangle$ are the right and left boundary spins.

In the large-N limit, T^N tends towards the projector onto the eigenspace spanned by the eigenvector belonging to the largest eigenvalue

$$|\lambda_+\rangle = \lim_{N\to\infty} \frac{T^N \, |\sigma\rangle}{\left\| T^N \, |\sigma\rangle \right\|}. \tag{1.19}$$

Eq. 1.19 is true for any $|\sigma\rangle$ that is not orthogonal to $|\lambda_+\rangle$.

The physical significance of the normalized lowest-lying eigenvector $|\lambda_1\rangle$ is that $\langle \lambda_1 | \uparrow \rangle$ and $\langle \lambda_1 | \downarrow \rangle$ represent the Boltzmann weight of $|\uparrow\rangle$ and $|\downarrow\rangle$ at the boundary of a half-infinite chain.

1.2.2 2D Ising model

Next, we treat the two-dimensional, square-lattice Ising model, which was solved in 1944 by Onsager [9] in a groundbreaking effort[1]. The energy function is still written as in Eq. 1.6, but now every lattice site has four neighbors.

[1] Onsager's solution rigorously showed, for the first time, that phase transitions could appear in simple statistical models and remained for a long time the only exactly solved model exhibiting critical behaviour. For a historical overview, see [10].

Let N be the number of columns and l be the number of rows of the lattice, and assume $l \gg N$. In the vertical direction, we apply periodic boundary conditions, as in the one-dimensional case. In the horizontal direction, we keep an open boundary. We refer to N as the system size.

Similarly as in the 1D case, the partition function can be written as

$$Z_N = \sum_{\boldsymbol{\sigma}} \prod_{\langle i,j,k,l \rangle} W(\sigma_i, \sigma_j, \sigma_k, \sigma_l) \tag{1.20}$$

where the product runs over all groups of four spins sharing the same face. The Boltzmann weight of such a face is given by

$$W(\sigma_i, \sigma_j, \sigma_k, \sigma_l) = \exp\left\{\frac{K}{2}(\sigma_i\sigma_j + \sigma_j\sigma_k + \sigma_k\sigma_l + \sigma_l\sigma_i)\right\} \tag{1.21}$$

We can express the Boltzmann weight of a configuration of the whole lattice as a product of the Boltzmann weights of the rows

$$Z_N = \sum_{\boldsymbol{\sigma}} \prod_{r=1}^{l} W(\sigma_1^r, \sigma_2^r, \sigma_1^{r+1}, \sigma_2^{r+1}) \ldots W(\sigma_{N-1}^r, \sigma_N^r, \sigma_{N-1}^{r+1}, \sigma_N^{r+1}) \tag{1.22}$$

where σ_i^r denotes the value of the ith spin of row r.

Now, we can generalize the definition of the transfer matrix to two dimensions, by defining it as the Boltzmann weight of an entire row

$$T_N(\boldsymbol{\sigma}, \boldsymbol{\sigma'}) = W(\sigma_1, \sigma_2, \sigma_1', \sigma_2') \ldots W(\sigma_{N-1}, \sigma_N, \sigma_{N-1}', \sigma_N') \tag{1.23}$$

If we take the spin configurations of an entire row as basis vectors, T_N can be written as a matrix of dimensions $2^N \times 2^N$.

Similarly as in the one-dimensional case, the partition function now becomes

$$Z_N = \sum_{\boldsymbol{\sigma}} \prod_{r=1}^{l} T_N(\boldsymbol{\sigma}^r, \boldsymbol{\sigma}^{r+1}) = \operatorname{Tr} T_N^l \tag{1.24}$$

In the limit of an $N \times \infty$ cylinder, the partition function is once again determined by the largest eigenvalue[2].

$$Z_N = \lim_{l\to\infty} T_N^l = \lim_{l\to\infty} (\lambda_0)_N^l \tag{1.25}$$

[2]As in the 1D case, T is symmetric, so it is orthogonally diagonalizable.

The partition function in the thermodynamic limit is given by

$$Z = \lim_{N \to \infty} Z_N \tag{1.26}$$

1.3 Partition function of the 2D Ising model as a tensor network

In calculating the partition function of 1D and 2D lattices, matrices of Boltzmann weights like W and T play a crucial role. We have formulated them in a way that is valid for any interaction-round-a-face (IRF) model, defined by

$$H \propto \sum_{\langle i,j,k,l \rangle} W(\sigma_i, \sigma_j, \sigma_k, \sigma_l), \tag{1.27}$$

where the summation is over all spins sharing a face. W can contain 4-spin, 3-spin, 2-spin and 1-spin interaction terms. The Ising model is a special case of the IRF model, with W given by Eq. 1.21.

We will now express the partition function of the 2D Ising model as a tensor network. The transfer matrix T is redefined in the process. This allows us to visualize the equations in a way that is consistent with the many other tensor network algorithms under research today. For an introduction to tensor network notation, see ??.

1.3.1 Tensor network of the partition function of a system of four spins

We define

$$Q(\sigma_i, \sigma_j) = \exp(K \sigma_i \sigma_j) \tag{1.28}$$

as the Boltzmann weight of the bond between σ_i and σ_j. It is the same as the 1D transfer matrix in Eq. 1.9.

The Boltzmann weight of a face W decomposes into a product of Boltzmann weights of bonds

$$W(\sigma_i, \sigma_j, \sigma_k, \sigma_l) = Q(\sigma_i, \sigma_j) Q(\sigma_j, \sigma_l) Q(\sigma_l, \sigma_k) Q(\sigma_k, \sigma_i). \tag{1.29}$$

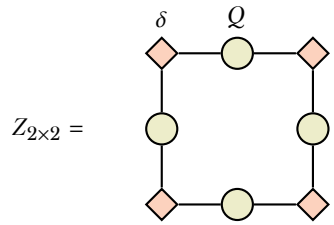

Figure 1.1: A tensor network representation of the partition function of the Ising model on a 2×2 lattice. See Eq. 1.30.

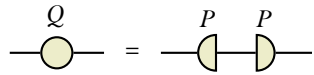

Figure 1.2: Graphical form of Eq. 1.32.

It is now easy to see that the partition function is equal to the contracted tensor network in Fig. 1.1:

$$\begin{aligned} Z_{2\times 2} &= \sum_{\sigma_1,\sigma_2,\sigma_3,\sigma_4} \sum_{a,b,c,d} \delta_{\sigma_1,a} Q(a,b) \delta_{\sigma_2,b} Q(b,c) \delta_{\sigma_3,c} Q(c,d) \delta_{\sigma_4,d} Q(d,a) \\ &= \sum_{\sigma_1,\sigma_2,\sigma_3,\sigma_4} W(\sigma_1,\sigma_2,\sigma_3,\sigma_4). \end{aligned} \tag{1.30}$$

where the Kronecker delta is defined as usual:

$$\delta_{ij} = \begin{cases} 1 & \text{if } i = j \\ 0 & \text{if } i \neq j. \end{cases} \tag{1.31}$$

1.3.2 Thermodynamic limit

We define the matrix P by

$$P^2 = Q. \tag{1.32}$$

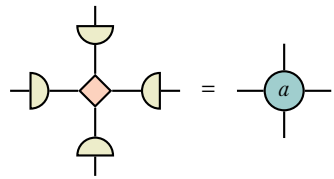

Figure 1.3: Graphical form of Eq. 1.33.

as in Fig. 1.2. This allows us to write the partition function of an arbitrary $N \times l$ square lattice as a tensor network of a single recurrent tensor a_{ijkl}, given by

$$a_{ijkl} = \sum_{a,b,c,d} \delta_{abcd} P_{ia} P_{jb} P_{kc} P_{ld}, \tag{1.33}$$

where the generalization of the Kronecker delta is defined as

$$\delta_{i_1 \ldots i_n} = \begin{cases} 1 & \text{if } i_1 = \ldots = i_n \\ 0 & \text{otherwise.} \end{cases} \tag{1.34}$$

See Fig. 1.3 and Fig. 1.4. At the edges and corners, we define suitable tensors of rank 3 and 2, which we will also denote by a:

$$a_{ijk} = \sum_{abc} \delta_{abc} P_{ia} P_{jb} P_{kc},$$
$$a_{ij} = \sum_{ab} \delta_{ab} P_{ia} P_{jb}.$$

The challenge is to approximate this tensor network in the thermodynamic limit.

1.3.3 The transfer matrix as a tensor network

With our newfound representation of the partition function as a tensor network, we can redefine the row-to-row transfer matrix from Eq. 1.23 as the

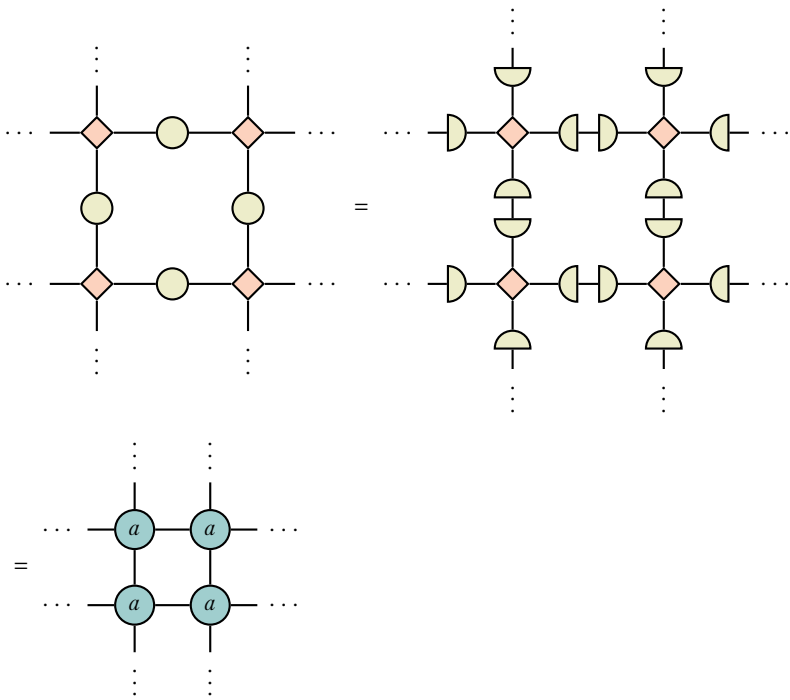

Figure 1.4: $Z_{N\times l}$ can be written as a contracted tensor network of $N \times l$ copies of the tensor a.

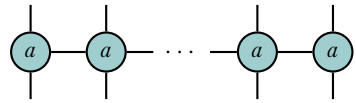

Figure 1.5: The definition of T_N as a network of N copies of the tensor a.

tensor network expressed in Fig. 1.5. For all l, it is still true that

$$Z_{N\times l} = \mathrm{Tr}\, T_N^l = \sum_{i=1}^{2^N} \lambda_i^l, \tag{1.35}$$

so the eigenvalues must be the same. That means that the new definition of the transfer matrix is related to the old one by a basis transformation

$$T_{\mathrm{new}} = P T_{\mathrm{old}} P^T. \tag{1.36}$$

1.4 Transfer matrix renormalization group

There is a deep connection between quantum mechanical lattice systems in d dimensions and classical lattice systems in $d+1$ dimensions. Via the imaginary time path integral formulation, the partition function of a one-dimensional quantum system can be written as the partition function of an effective two-dimensional classical system. The ground state of the quantum system corresponds to the largest eigenvector of the transfer matrix of this corresponding classical system.

For more on the quantum-classical correspondence, see ??.

1.4.1 The infinite system algorithm for the transfer matrix

Nishino [1, 2] was the first to apply density matrix renormalization group methods in the context of two-dimensional classical lattices.

Analogous to the infinite system DMRG algorithm for approximating the Hamiltonian of quantum spin chains, our goal is to approximate the transfer matrix in the thermodynamic limit as well as possible within a restriced number of basis states m. We will do this by adding a single site at a time, and truncating the dimension from $2m$ to m at each iteration.

For simplicity, we assume that, at the start of the algorithm, the transfer matrix already has dimension m. We call this transfer matrix P_N.

We note that this initial P_N for a system with a free boundary can be obtained by contracting a-tensors, until P_N becomes of size $m \times m$. See Fig. 1.6.

To specify fixed instead of open boundary conditions, we may use as boundary tensor a slightly modified version of the three-legged version of a, namely

$$a^{\sigma}_{ijk} = \sum_{abc} \delta_{\sigma abc} P_{ia} P_{jb} P_{kc}, \tag{1.37}$$

that represents an edge site with spin fixed at σ.

We enlarge the system with one site by contracting with an additional a-tensor, obtaining P_{N+1}. See the first network in Fig. 1.7.

In order to find the best projection from $2m$ basis states back to m, we embed the system in an environment that is the mirror image of the system we presently have. We call this matrix T_{2N+2}. It represents the transfer matrix of $2N+2$ sites. We find the largest eigenvalue and corresponding eigenvector, as shown in Fig. 1.8.

The equivalent of the *reduced density matrix of a block* in the classical case is:

$$\rho_{N+1} = \sum_{\sigma_B} \langle \sigma_B | \lambda_0 \rangle \langle \lambda_0 | \sigma_B \rangle , \tag{1.38}$$

where we have summed over all the degrees of freedom of one of the half-row transfer matrices P_{N+1}. See the first step of Fig. 1.9.

The optimal renormalization

$$\widetilde{P}_{N+1} = O P_{N+1} O^{\dagger} \tag{1.39}$$

is obtained by diagonalizing ρ_{N+1} and keeping the eigenvectors corresponding to the m largest eigenvalues. See the second step of Fig. 1.9.

With this blocking procedure, we can successively find

$$P_{N+1} \to P_{N+2} \to \ldots, \tag{1.40}$$

until we have reached some termination condition.[3]

[3] The termination condition for the infinite-system algorithm is discussed in ??.

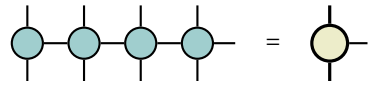

Figure 1.6: A good starting point for the half-row transfer P_N is obtained by contracting a couple of a-tensors, until P_N reaches dimension m.

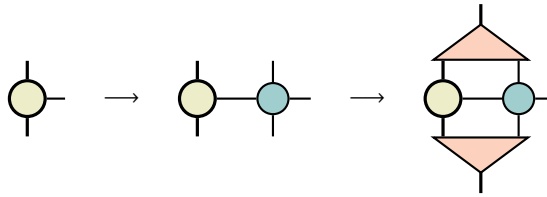

Figure 1.7: In the first step, P_{N+1} is obtained by contracting the current half-row transfer matrix P_N with an additional a-tensor. In the second step, P_{N+1} is truncated back to an m-dimensional matrix, with the optimal low-rank approximation given by keeping the basis states corresponding to the m largest eigenvalues of the density matrix. See Fig. 1.9.

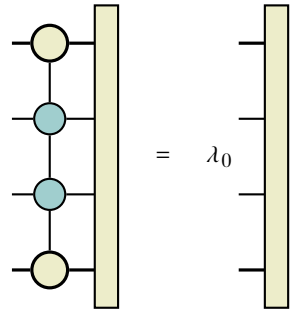

Figure 1.8: Equation for the lowest-lying eigenvector of the row-to-row transfer matrix T_{2N+2}.

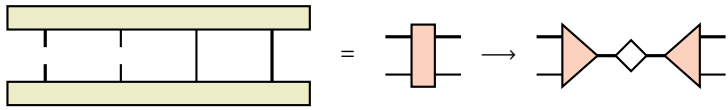

Figure 1.9: Graphical form of Eq. 1.38. In the second step, ρ_{N+1} is diagonalized and only the eigenvectors corresponding to the m largest eigenvalues are kept.

1.4.2 Physical interpretation of the reduced density matrix

Generalizing the remarks from section 1.2.1.1 to the two-dimensional case, we see that the normalized lowest-lying eigenvector of the transfer matrix T_N contains the Boltzmann weights of spin configurations on the boundary of a half-infinite $N \times \infty$ lattice.

Therefore, the classical equivalent of the quantum mechanical reduced density matrix, given by Eq. 1.38, and by the first network in Fig. 1.9, represents the Boltzmann weights of configurations along a cut in an $N \times \infty$ lattice.

Nishino and Okunishi [2], drawing on ideas from Baxter, realized the Boltzmann weights of configurations along this cut could be obtained by employing *corner transfer matrices*, making it unneccessary to solve the eigenvalue problem in Fig. 1.8. Their method, called the Corner Transfer Matrix Renormalization Group method, consumes far less resources while maintaining precision. For this reason, it is the method of choice for most of the simulations in this thesis.

1.5 Corner transfer matrix renormalization group

1.5.1 Corner transfer matrices

The concept of corner transfer matrices for 2D lattices was first introduced by Baxter [3–5]. Whereas the row-to-row transfer matrix Eq. 1.23 corresponds to adding a row to the lattice, the corner transfer matrix adds a quadrant of spins. It was originally defined by Baxter as

$$A_{\boldsymbol{\sigma},\boldsymbol{\sigma}'} = \begin{cases} \sum \prod_{\langle i,j,k,l \rangle} W(\sigma_i, \sigma_j, \sigma_k, \sigma_l) & \text{if } \sigma_1 = \sigma_1' \\ 0 & \text{if } \sigma_1 \neq \sigma_1'. \end{cases} \tag{1.41}$$

Here, the product runs over groups of four spins that share the same face, and the sum is over all spins in the interior of the quadrant.

In a symmetric and isotropic model such as the Ising model, we have

$$W(a,b,c,d) = W(b,a,d,c) = W(c,a,d,b) = W(d,c,b,a) \tag{1.42}$$

and the partition of an $N \times N$ lattice is expressed as

$$Z_{N\times N} = \mathrm{Tr}\, A^4 = \sum_{\alpha=1}^{2^N} \nu_\alpha^4, \tag{1.43}$$

where ν_α are the eigenvalues of A.

In the thermodynamic limit, this partition function is equal to the partition function of an $N \times \infty$ lattice, given by Eq. 1.24.

1.5.2 Corner transfer matrix as a tensor network

Similarly to how we redefined the row-to-row transfer matrix (Eq. 1.23) as the tensor network in Fig. 1.5, we can redefine the corner transfer matrix (Eq. 1.41) as the tensor network in Fig. 1.10. Again, the new and old definitions of A are related by a basis tranformation

$$A_{\text{new}} = P A_{\text{old}} P^T. \tag{1.44}$$

The partition function, as in Eq. 1.43, is given by the tensor network in Fig. 1.11.

1.5.3 Corner transfer matrix renormalization group method

The corner transfer matrix renormalization group iteratively adds a layer to A, while keeping only m basis states at each step. It was first employed by Baxter [4, 5].

As can be seen from Eq. 1.43, the best approximation to the partition function within a restricted number of basis states m is obtained by keeping the eigenvectors corresponding to the m largest eigenvalues of A^4.

The algorithm proceeds very much like the transfer matrix renormalization group method. In addition to renormalizing the half-row transfer matrix P, we also renormalize the corner transfer matrix A at each step, using the projector obtained from diagonalizing A^4 or equivalently A.

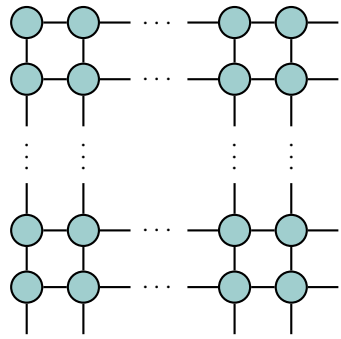

Figure 1.10: Corner transfer matrix expressed as a contraction of a-tensors.

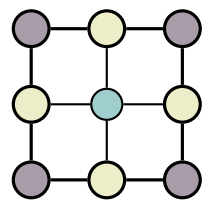

Figure 1.11: Tensor network approximation to $Z_{N\times N}$ in the CTMRG method.

We first initialize P_N and A_N. A free or fixed boundary may be imposed in the same way as in the transfer matrix renormalization group. See Eq. 1.37.

We then obtain the unrenormalized A_{N+1} by adding a layer of spins to the quadrant represented by A_N. This is done by contracting with two half-row transfer matrices P_N and a single a-tensor, as shown in the first step of Fig. 1.12. We obtain the unnormalized P_{N+1} as before, as shown in the first step of Fig. 1.7.

We use the projector to obtain the renormalized versions of A_{N+1} and T_{N+1}

$$\widetilde{A}_{N+1} = OA_{N+1}O^\dagger, \tag{1.45}$$

$$\widetilde{T}_{N+1} = OT_{N+1}O^\dagger. \tag{1.46}$$

shown in the second steps of Fig. 1.12 and Fig. 1.7.

We repeat the above procedure to successively obtain

$$A_{N+1} \to A_{N+2} \to \ldots, \tag{1.47}$$

$$T_{N+1} \to T_{N+2} \to \ldots \tag{1.48}$$

until a convergence criterion is reached.

1.5.3.1 Equivalence to TMRG and DMRG in the thermodynamic limit

A^4 contains the Boltzmann weights of spins along a cut in the middle of the $N \times N$ system. In contrast, the matrix in Eq. 1.38 contains the Boltzmann weights of spins along a cut down the middle of an $N \times \infty$ system.

In the thermodynamic limit, both become the same, and we can make the identification

$$\rho = A^4. \tag{1.49}$$

See Fig. 1.13.

Hence, DMRG and TMRG are equivalent to CTMRG in the thermodynamic limit. This was first realized by Nishino [11].

1.6 Calculation of observable quantities

1.6.1 Free energy per site

Baxter [4, 5] showed that the partition function per site

$$\kappa = Z^{1/N^2} \tag{1.50}$$

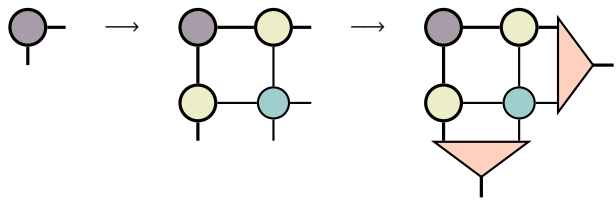

Figure 1.12: In the first step, the unrenormalized A_{N+1} is obtained by contracting with two copies of P_N and a single a-tensor. This corresponds to adding a layer of spins to the quadrant, thus enlarging it from $N \times N$ to $N+1 \times N+1$. In the second step, A_{N+1} is renormalized with the projector obtained from diagonalizing A^4_{N+1} and keeping the basis states corresponding to the m largest eigenvalues.

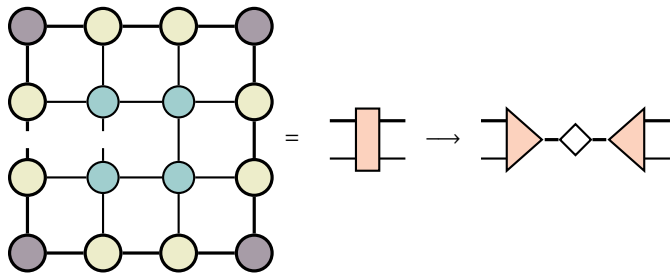

Figure 1.13: The matrix A^4_{N+1} is approximately equal to ρ_{N+1} in Eq. 1.38. Compare the graphical forms of this network and the one shown in Fig. 1.9. We obtain the optimal projector by diagonalizing A^4_{N+1}, or equivalently A_{N+1}.

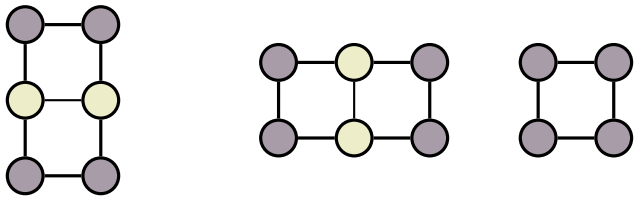

Figure 1.14: From left to right: r_2, r_3 and r_4 as in Eq. 1.51.

is, within the corner transfer matrix renormalization group method, written as

$$\kappa = \frac{r_1 r_4}{r_2 r_3}, \tag{1.51}$$

with r_2, r_3 and r_4 as in Fig. 1.14 and $r_1 = Z_{N\times N}$ as in Fig. 1.11. The free energy per site is then simply

$$\frac{F}{N^2} = -T \log \kappa. \tag{1.52}$$

1.6.2 Magnetization per site

The magnetization per site may be calculated as

$$M = T \frac{\partial(\log \kappa)}{\partial h}, \tag{1.53}$$

but this involves a numerical derivative and a numerical limit $h \to 0$ in the case of the spontaneous magnetization. A more practical method, that is employed in this thesis, is to use the magnetization of the central spin

$$\langle \sigma_0 \rangle = \frac{\sum_{\{\boldsymbol{\sigma}\}} \sigma_0 \exp\left(-\beta H(\boldsymbol{\sigma})\right)}{Z} \tag{1.54}$$

as a proxy quantity to the magnetization per site.

In the original definition of the corner transfer matrix by Baxter (Eq. 1.41), it is written as

$$\langle \sigma_0 \rangle = \frac{\mathrm{Tr} A_+^4 - \mathrm{Tr} A_-^4}{\mathrm{Tr} A^4}. \tag{1.55}$$

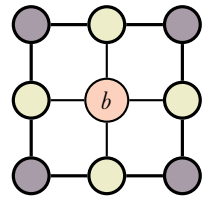

Figure 1.15: Unnormalized expectation value of central spin, with the tensor b_{ijkl} defined in Eq. 1.56.

Here, $A_\pm$ is the corner transfer matrix with the central spin fixed to $\pm$.

In tensor network notation, $\mathrm{Tr}\, A_+^4 - \mathrm{Tr}\, A_-^4$ is written as the tensor network in Fig. 1.15, with the tensor b_{ijkl} defined as

$$b_{ijkl} = \sum_{\sigma \in \{-1,1\}} \sigma \delta_{\sigma ijkl}. \tag{1.56}$$

All numerical results in this thesis involving the magnetization per site are actually obtained by calculating $\langle \sigma_0 \rangle$, which shall be referred to simply as M from now on.

1.6.3 Analogy to entanglement entropy for classical systems

The key point of the corner transfer matrix renormalization group method [2, 11] is that it unifies White's density matrix renormalization group method [6] with Baxter's corner transfer matrix approach [3, 4], through the identification (in the isotropic case)

$$\rho_{\text{half-chain}} = A^4. \tag{1.57}$$

This allows one to define a 2D classical analogue to the half-chain entanglement entropy of a 1D quantum system

$$S_{\text{classical}} = -\,\mathrm{Tr}\, A^4 \log A^4 = -\sum_{\alpha=1}^{m} \nu_\alpha^4 \log \nu_\alpha^4, \tag{1.58}$$

where ν_α are the eigenvalues of the corner transfer matrix A. In the CTMRG algorithm, A is kept in diagonal form, making $S_{\text{classical}}$ trivial to compute.

In [12], numerical evidence is given for the validity of Eq. 1.58 for a wide range of models, and the concept is generalized to higher dimensions. For an overview of applying corner transfer matrices in higher dimensions and to quantum systems, see [13].

1.7 Spectrum of the corner transfer matrix

1.7.1 Analytical results for the Ising model

In what follows, we present results established in [14, 15].

For the off-critical Ising model on a square lattice, we have [16]

$$\hat{\rho} = \hat{A}^4 = \exp(-\hat{H}_{\mathrm{CTM}}), \tag{1.59}$$

where

$$\hat{H}_{\mathrm{CTM}} = \sum_{l=0}^{\infty} \epsilon_l(T) c_l^\dagger c_l, \tag{1.60}$$

with c_l and $c_l^\dagger$ fermionic annihilation and creation operators and

$$\epsilon_l = \begin{cases} (2l+1)\epsilon(T) & \text{if } T > T_c, \\ 2l\epsilon(T) & \text{if } T < T_c. \end{cases} \tag{1.61}$$

with $\epsilon(T)$ a model-specific factor that only depends on temperature.

In other words, the reduced density matrix (or equivalently, the corner transfer matrix A) can be written as a density matrix of an effective free fermionic Hamiltonian with equally spaced excitations.

What does this mean for the spectrum of A? If we assume a free boundary, we have to distinguish between the ordered and disordered phase.

In the disordered phase, we have $\epsilon_l = (2l+1)\epsilon(T)$. The ground state, $E = 0$, corresponds to the vacuum state of the effective system described by H_{CTM}. The single-fermion excitations give ϵ, 3ϵ, 5ϵ, ..., while two-fermion excitations give 4ϵ ($c_0^\dagger c_1^\dagger |0\rangle$), 6ϵ ($c_0^\dagger c_2^\dagger |0\rangle$) and 8ϵ ($c_0^\dagger c_3^\dagger |0\rangle$ *or* $c_1^\dagger c_2^\dagger |0\rangle$). So the first degeneracy appears at 8ϵ. 9ϵ is also degenerate: it can be constructed with a single-fermion excitation ($c_4^\dagger |0\rangle$) and a three-fermion excitation ($c_2^\dagger c_1^\dagger c_0^\dagger |0\rangle$).

The numerical results from the CTMRG algorithm exactly confirm this picture. See the $T = 2.6$ line in the left panel of Fig. 1.16. The gap after the

first two eigenvalues is due to the absence of the level 2ϵ. The ϵ_l are linear and the degeneracies are correct.

In the ordered phase, we have a two-fold degeneracy for every state due to symmetry and ground state energy $E = 0$. After that, the only available levels are 2ϵ, 4ϵ, 6ϵ, ... The degeneracy of the nth energy level is given by $2p(n)$, twice the number of partitions of n into distinct integers [17], with the factor of two coming from symmetry.

To illustrate: $c_1^\dagger c_2^\dagger |0\rangle$ and $c_3^\dagger |0\rangle$ both have $E = 6\epsilon$, the third energy level (counting the vacuum as the zeroth energy level), which is to say $p(3) = 2$ since $\{3, 2 + 1\}$ are the ways to write 3. The line $T = 2$ in the left panel of Fig. 1.16 confirms these results.

With a fixed boundary, the spectrum in the disordered phase doesn't change. In the ordered phase however, the two-fold degeneracy due to symmetry is lifted, so the degeneracy of the nth energy level becomes $p(n)$. As a consequence, the spectrum decays much faster. See the right panel of Fig. 1.16.

At or close to criticality, the expression in Eq. 1.59 breaks down, and the spectrum of $\hat{\rho}$ is smoothened out. In general, below and at criticality, the spectrum decays slower for a free boundary. This is to be expected, since A preserves the symmetry when the boundary is free. At $T = 0$, A has two equally large non-zero eigenvalues, representing either all up or all down spins on the boundary of the quadrant, while for a fixed boundary, A has one non-zero eigenvalue: it represents a completely polarized state.

1.7.2 Implications for finite-m simulations

When approximating the corner transfer matrix with a free boundary in the ordered phase, it is crucial to retain all basis states corresponding to an energy level [17]. Failure to do so will lead to a symmetry-broken state.

Near criticality, however, even when all degenerate basis states are kept, the algorithm is still prone to symmetry breaking.

1.8 Equivalence to variational approximation in the space of matrix product states.

In closing this chapter, we note that it has been widely established that DMRG produces a ground state that corresponds to a variational optimization within a matrix-product structure [18, 19].

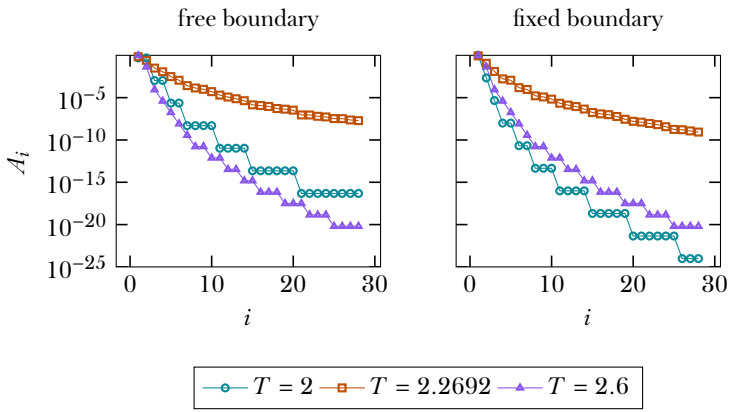

Figure 1.16: First part of the spectrum of A after $n = 1000$ steps with a bond dimension of $m = 250$.

CTMRG and TMRG, by the classical-quantum equivalence, find transfer matrices with similar structure. This was first noted by Baxter [5].

For an introduction to these algorithms from this variational point of view, see [20].

Bibliography

[1] T. Nishino, "Density matrix renormalization group method for 2D classical models", Journal of the Physical Society of Japan **64**, 3598–3601 (1995).

[2] T. Nishino, and K. Okunishi, "Corner transfer matrix renormalization group method", Journal of the Physical Society of Japan **65**, 891–894 (1996).

[3] R. J. Baxter, "Dimers on a rectangular lattice", Journal of Mathematical Physics **9**, 650–654 (1968).

[4] R. J. Baxter, "Variational approximations for square lattice models in statistical mechanics", Journal of Statistical Physics **19**, 461–478 (1978).

[5] R. J. Baxter, *Exactly solved models in statistical mechanics* (Elsevier, 1982) Chap. 13.

[6] S. R. White, "Density matrix formulation for quantum renormalization groups", Physical Review Letters **69**, 2863 (1992).

[7] D. Tong, *Lectures on statistical physics*, (2011) `http://www.damtp.cam.ac.uk/user/tong/statphys.html` (visited on 06/07/2017).

[8] E. Ising, "Beitrag zur theorie des ferromagnetismus", Zeitschrift für Physik **31**, 253–258 (1925).

[9] L. Onsager, "Crystal statistics. I. a two-dimensional model with an order-disorder transition", Phys. Rev. **65**, 117–149 (1944).

[10] S. M. Bhattacharjee, and A. Khare, "Fifty years of the exact solution of the two-dimensional ising model by onsager", Current Science **69**, 816–821 (1995).

[11] T. Nishino, and K. Okunishi, "Corner transfer matrix algorithm for classical renormalization group", Journal of the Physical Society of Japan **66**, 3040–3047 (1997).

[12] C.-Y. Huang, T.-C. Wei, and R. Orús, "Holographic encoding of universality in corner spectra", Physical Review B **95**, 195170 (2017).

[13] R. Orús, "Exploring corner transfer matrices and corner tensors for the classical simulation of quantum lattice systems", Physical Review B **85**, 205117 (2012).

[14] I. Peschel, and V. Eisler, "Reduced density matrices and entanglement entropy in free lattice models", Journal of Physics A: Mathematical and Theoretical **42**, 504003 (2009).

[15] I. Peschel, M. Kaulke, and Ö. Legeza, "Density-matrix spectra for integrable models", Annalen der Physik **8**, 153–164 (1999).

[16] B. Davies, "Corner transfer matrices for the Ising model", Physica A: Statistical Mechanics and its Applications **154**, 1–20 (1988).

[17] K. Okunishi, Y. Hieida, and Y. Akutsu, "Universal asymptotic eigenvalue distribution of density matrices and corner transfer matrices in the thermodynamic limit", Physical Review E **59**, R6227 (1999).

[18] S. Östlund, and S. Rommer, "Thermodynamic limit of density matrix renormalization", Physical Review Letters **75**, 3537 (1995).

[19] S. Rommer, and S. Östlund, "Class of ansatz wave functions for one-dimensional spin systems and their relation to the density matrix renormalization group", Physical Review B **55**, 2164 (1997).

[20] T. Nishino, T. Hikihara, K. Okunishi, and Y. Hieida, "Density matrix renormalization group: introduction from a variational point of view", International Journal of Modern Physics B **13**, 1–24 (1999).